Cambridge Centre for Computational Chemical Engineering

University of Cambridge

Department of Chemical Engineering

Preprint ISSN 1473 – 4273

Bivariate Stochastic Modelling of Nanoparticles

Clive Wells, Neal Morgan, Markus Kraft[1], and Wolfgang Wagner[2]

submitted: 1st June 2004

[1] Department of
Chemical Engineering
University of Cambridge
Pembroke Street
Cambridge CB2 3RA
UK
E-Mail: markus_kraft@cheng.cam.ac.uk

[2] Weierstrass Institute
for Applied Analysis
and Stochastics
Mohrenstraße 39
D - 10117 Berlin
Germany
E-Mail: wagner@wias-berlin.de

Preprint No. 23

c4e

Key words and phrases. Nanoparticles, laminar flames, particle growth, stochastic simulation.

Edited by
Cambridge Centre for Computational Chemical Engineering
Department of Chemical Engineering
University of Cambridge
Cambridge CB2 3RA
United Kingdom.

Fax: + 44 (0)1223 334796
E-Mail: c4e@cheng.cam.ac.uk
World Wide Web: http://www.cheng.cam.ac.uk/c4e/

Abstract

In this paper we find numerical solutions to a generalization of Smoluchowski's coagulation equation using a bivariate mass-flow stochastic algorithm. Specifically we simulate the growth and morphology of nanoparticles in premixed laminar flames. The our model includes terms for particle inception, surface growth and particle sintering. A test simulation was implemented to examine the stochastic algorithm under various simple starting conditions. The production of SiO_2 from a low-pressure premixed laminar flame doped with SiH_4 was investigated. A free-molecular kernel was used for the coagulation terms and a grain boundary diffusion model implemented for the particle sintering. The flame itself was simulated using a skeletal $H_2/O_2/Ar$ mechanism including the SiH_4 oxidation reactions. We were able to simulate the transition from a bimodal particle size distribution to a unimodal particle size distribution for the silica particles produced, and predict a value for an effective fractal dimension of silica particles in a flame close to those reported in the experimental literature.

Contents

1 Introduction

The use of nano particles in industry is becoming more widespread since the physical properties they possess may be different from those of the bulk material. As such, the ability to model the particle size distribution (PSD) is extremely important as the size and shape of the particles may affect the physical attributes of the final product. The use of population balance models to study nano particle growth has become more established, especially when studying metal oxides formed in flames [1, 2]. These models of particle systems tend to focus on coagulation and particle inception as this keeps the simulation simple, however these mechanisms alone may not be sufficient to describe the full particle dynamics of the system accurately. Most previous simulations have only tracked particle mass. Additional mechanisms, for example sintering, can be incorporated into the simulation in order to describe the surface area evolution.

Finite element methods have been used to generate numerical solutions to the sintering-coagulation equation [3] but the exceedingly high computational expense of this technique makes it grossly impractical as a simulation method. Stochastic particle methods allow us to simulate this bivariate distribution without such computational expense [4, 5, 6] and allow us to extend the model to include other particle growth mechanisms. We add a term to the Smoluchowski coagulation equation that describes the deposition of new mass onto the surface of particles. This addition, along with particle sintering represents a more accurate model than inception and coagulation alone.

In this paper we make use of a mass-flow algorithm [7, 8, 9] to study the evolution of the particle system over time. To derive the mass-flow algorithm, we write Smoluchowski's equation in terms of the mass density rather than the number density. Previous studies [5, 8] have shown that the mass-flow algorithm offers some computational advantages over the direct simulation algorithm (Marcus-Lushnikov process; [10, 11]).

This paper is arranged as follows. In section 2 we introduce an extended form of Smoluchowski's coagulation equation and discuss the sintering term. Section 3 introduces a simple simulation to test the algorithm and in section 4 we simulate a flame producing silica particles.

2 A Generalization of Smoluchowski's Coagulation Equation

In order to model the growth and morphology of the particles within the system, we extend Smoluchowski's coagulation equation to include extra terms for particle

inception, surface growth and particle sintering:

$$\begin{aligned}\frac{\partial}{\partial t}n_t(v,a) = &\frac{\partial}{\partial a}\left(\frac{1}{t_0}\left[a - a_0\left(\frac{v}{v_0}\right)^{2/3}\right]n_t(v,a)\right)\\ &+\frac{1}{2}\int_{v_0}^{v}\int_{a_0\left(\frac{v'}{v_0}\right)^{2/3}}^{\frac{a_0 v'}{v_0}}\beta_{v',v-v'}(a',a-a')n_t(v',a')n_t(v-v',a-a')\,\mathrm{d}a'\,\mathrm{d}v'\\ &-n_t(v,a)\int_{v_0}^{\infty}\int_{a_0\left(\frac{v'}{v_0}\right)^{2/3}}^{\frac{a_0 v'}{v_0}}\beta_{v,v'}(a,a')n_t(v',a')\,\mathrm{d}a'\,\mathrm{d}v'\\ &+I^{\text{incep}}n^{in} + I^{\text{surf}}\left[(a-a_0)n_t(v-v_0,a-a_0) - an_t(v,a)\right] \quad (1)\end{aligned}$$

with the initial condition $n_0(v,a)$. The number of particles of volume, v, and area, a, at a time, t, is denoted by $n_t(v,a)$. The first term on the right hand side of equation (1) describes the loss of surface area of a particle due to sintering. The parameter t_0 is the characteristic sintering time and takes the form of a function of particle diameter d_p and temperature T. The zero subscript denotes the smallest particle that can exist in the system. The second and third terms describe how the particles in the system coagulate together. The coagulation kernel, $\beta_{v,v'}(a,a')$ determines the probability with which any two particles will coagulate. The fourth term describes a source of new particles into the system. The rate at which this occurs, I^{incep} comes from, in the case of flames, the chemical rate of production of the simulated species. Finally the fifth term describes how particles grow by the deposition of new mass directly onto the surface of an existing particle. Again, in the case of flames, the rate of this process, I^{surf} comes from the gas phase kinetics.

There are many mechanisms to describe particle sintering and its rate. In this paper, we make use of a boundary diffusion model that calculates the characteristic sintering time as

$$t_0 = A_{\text{sint}}Td_p^4\exp\left(\frac{B_{\text{sint}}}{T}\right), \quad (2)$$

where A_{sint} and B_{sint} are species-dependent constants, T is the temperature and d_p the particle diameter. The calculation of particle diameter brings its own problems. In some papers, a very simple calculation of diameter is performed such that $d_p = 6v/a$. This formula works well for a spherical particle, but has the unfortunate consequence that a partially sintered particle has a calculated diameter less than that of a fully sintered one. This is counter intuitive. In this paper we make use of the collision cross-section to determine the particle diameter.

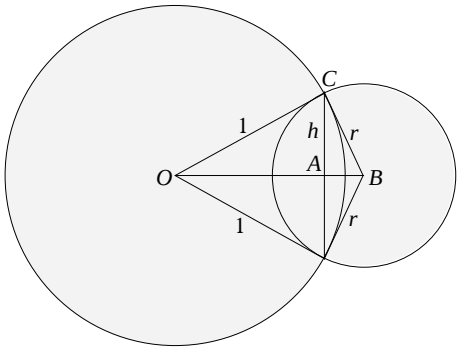

Figure 1: A schematic representation of the collision cross section.

Consider two spheres of diameter 1 and r ($r \leqslant 1$) that are touching (fig 1). The projected view is the union of two discs. Let us call the projected distance between the centres of the discs, $D = OB$. The cross sectional ares is

$$A(r, D) = \frac{1}{2}\pi(1 + r^2) + \sin^{-1} d_1 + r^2 \sin^{-1} \frac{d_2}{r} + d_1\sqrt{1 - d_1^2} + d_2\sqrt{r^2 - d_2^2}, \quad (3)$$

for $r > 1 - D$, where,

$$d_1 = \frac{1}{2}\left(D + \frac{1 - r^2}{D}\right) \quad \text{and} \quad d_2 = \frac{1}{2}\left(D - \frac{1 - r^2}{D}\right). \quad (4)$$

In the case where $r \leqslant 1 - D$, the smaller sphere is completely obscured by the larger. In this case, $A(r, D) = \pi$.

The point of contact between the spheres lies uniformly on the unit sphere. Let us use spherical polar coordinates θ, ϕ with the z-axis along the line of projection. The apparent distance between the spheres is $D = (1 + r)\sin\theta$. Thus the average collision cross-section $\Sigma(r)$ is

$$\begin{aligned}
\Sigma(r) &= \frac{1}{4\pi}\int A(r, (1 + r)\sin\theta)\ \mathrm{d}\Omega & (5)\\
&= \int_0^{\frac{\pi}{2}} A(r, (1 + r)\sin\theta)\sin\theta\ \mathrm{d}\theta & (6)\\
&= \frac{\pi}{1 + r}\left(1 - \sqrt{r}\right)^2 \\
&\quad + \int_{\sin^{-1}\left(\frac{1-r}{1+r}\right)}^{\frac{\pi}{2}} \sin\theta\left(\frac{1}{2}\pi(1 + r^2) + \sin^{-1} d_1 + r^2 \sin^{-1}\frac{d_2}{r}\right. \\
&\qquad \left. + d_1\sqrt{1 - d_1^2} + d_2\sqrt{r^2 - d_2^2}\right)\mathrm{d}\theta & (7)
\end{aligned}$$

This is not simple to compute. However the $r = 1$ case is done easily, corresponding to the coagulation of identical spherical particles. In this case $D = 2r\sin\theta = 2d_1 =$

$2d_2$. We have

$$\begin{aligned}\Sigma(1) &= \int_0^{\frac{\pi}{2}} \sin\theta(\pi + 2\theta + 2\sin\theta\cos\theta)\,\mathrm{d}\theta &(8)\\ &= \left[-\pi\cos\theta - 2\theta\cos\theta + 2\sin\theta + \tfrac{2}{3}\sin^3\theta\right]_0^{\frac{\pi}{2}} &(9)\\ &= \pi + \tfrac{8}{3}. &(10)\end{aligned}$$

The collision length $\bar{a}$ is determined by $\Sigma = \pi\bar{a}^2$ and is therefore given by $\bar{a} = \sqrt{1 + \frac{8}{3\pi}}$. We remark that $2^{\frac{1}{3}} < \bar{a} < 2^{\frac{1}{2}}$ which is to be expected, since the smaller bound corresponds to a spherical particle with the same total volume and the upper bound corresponds to the sum of the areas of the two individual particles (so no account is taken for one particle being partially obscured by the other).

Next we try to approximate $\bar{a}(r)$ by $\nu^\alpha\sigma^\beta$ where ν is the (scaled) volume and σ is the scaled surface area. For the coagulated particle we have $\nu = 1 + r^3$ and $\sigma = 1 + r^2$. We impose the condition that $\bar{a}(1) = \nu^\alpha\sigma^\beta$ as a constraint on α and β, leading to $2^{\alpha+\beta} = \bar{a}$. We also assume for dimensional reasons that $3\alpha + 2\beta = 1$. Therefore $2^{(1+\beta)/3} = \bar{a}$ leading to formulae for α and β,

$$\alpha = \log_2\left[2\left(1 + \frac{8}{3\pi}\right)^{-1}\right] \quad \text{and} \quad \beta = \log_2\left[\frac{1}{2}\left(1 + \frac{8}{3\pi}\right)^{\frac{3}{2}}\right]. \tag{11}$$

Thus the sintering time now becomes

$$t_0 = A_{\text{sint}} T v^{4\alpha} a^{4\beta} \exp\left(\frac{B_{\text{sint}}}{T}\right). \tag{12}$$

We use a bivariate form of the free molecular kernel to simulate particle collisions introduced by [12]. The kernel is given by

$$\beta_{v,v'}(a, a') = \left(\frac{kTa_0^2}{2\pi m_0}\right)^{\frac{1}{2}} K(x, x'), \tag{13}$$

where k is Boltzmann's constant, m_0 is the mass of a primary particle, $x = (\nu, \sigma) = (v/v_0, a/a_0)$ and $K(x, x')$ is a dimensionless function given by

$$K(x, x') = \left(\frac{1}{\nu} + \frac{1}{\nu'}\right)^{\frac{1}{2}} \left[(s(\nu)\sigma)^{\frac{1}{2}} + (s(\nu')\sigma')^{\frac{1}{2}}\right]^2. \tag{14}$$

The function $s(\nu)$ is the surface area accessability function and is given by

$$\begin{aligned} s(\nu) &= \lambda_1\nu^{\gamma-1} + \lambda_2;\\ \lambda_1 &= 2^{1-\gamma}(D_S - 2);\\ \lambda_2 &= 3 - D_S, \end{aligned} \tag{15}$$

where $D_S \in [2, 3]$ is a surface fractal dimension and $\gamma \in [0, 1]$ is the surface area scaling factor.

3 The Test Simulations

In order to produce numerical solutions to the model, we made use of a mass-flow stochastic algorithm developed in [5, 13]. This Monte Carlo algorithm has improved scaling properties compared to that developed by Tandon and Rosner [4], as the number of stochastic particles increases.

Test simulations were performed to show how the model deals with particle inception, coagulation, surface growth and sintering. Initially we set the surface growth rate to be constant at a value of 0.1 per unit area per unit time, and an initial concentration of unity. The parameters D_S and γ were set to 2.1 and 0.8 respectively. The initial number of stochastic particles was 8192 and the results averaged over 20 runs.

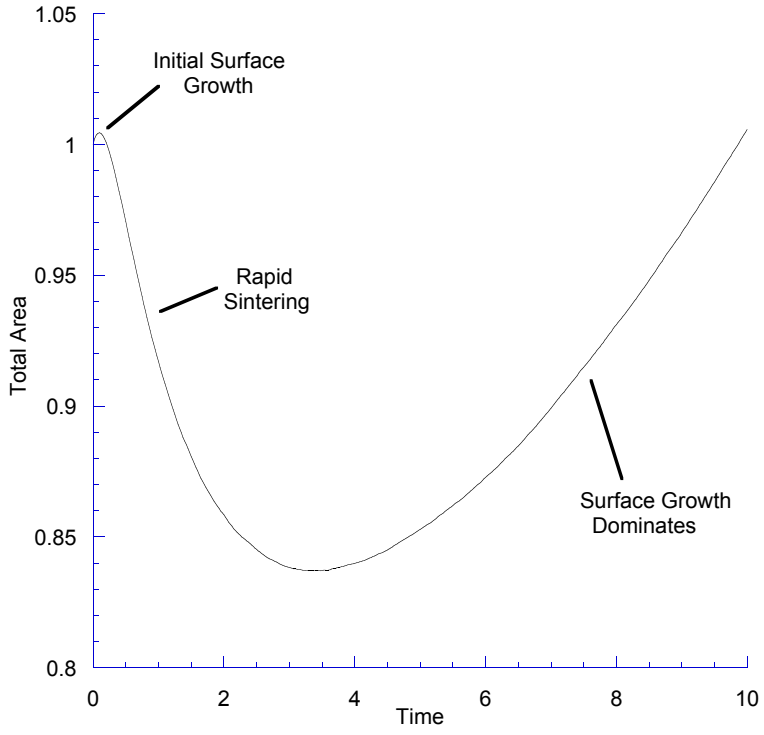

Figure 2: Total surface area for the first test simulation.

Figure 2 shows the evolution of the total area of a system of particles undergoing coagulation, sintering and surface growth. Note that the initial surface growth that occurs in the system ($t \leqslant 0.1$) is quickly suppressed as sintering becomes more prevalent. At around $t = 3.5$ the rate of sintering has slowed and the rate of surface growth has become faster due to the increased average size of the particles.

The second test simulation included a particle source rate of 0.1 per unit volume per unit time, in addition to surface growth, coagulation and sintering. Particle size distributions for this system at various times are shown in Fig. 3.

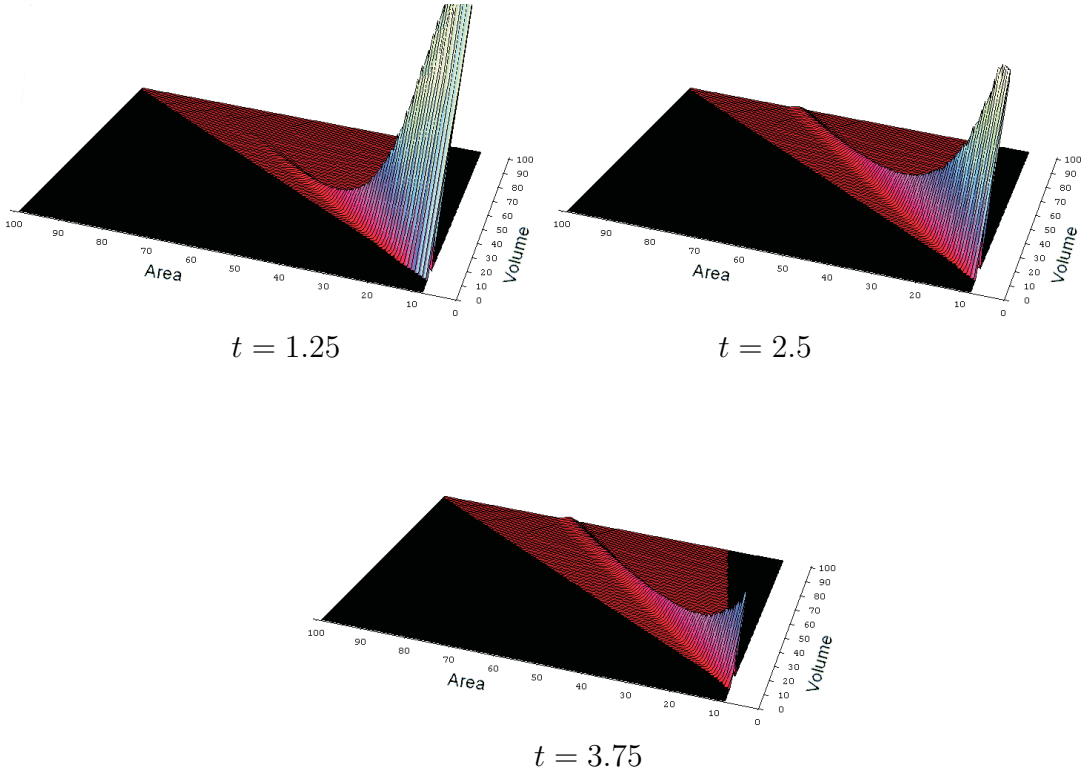

Figure 3: Evolution of the PSD at various times

One can see from Fig. 3 that the initial peak of small particles falls off rapidly to give a broadening of the distribution. Sintering can clearly be seen as a ridge in the PSD moving across the plot from left to right as the surface area is reduced. Initially the particles lie on the line of maximum surface area to the left of the diagrams.

4 Simulation of Silica Formation

We simulated the formation of SiO_2 particles from a low-pressure premixed laminar $H_2/O_2/Ar$ flame doped with SiH_4. The chemistry of the flame was calculated using reactions for an $H_2/O_2/Ar$ flame combined with a skeletal mechanism for the oxidation of SiH_4 as described in [1]. The flame was simulated using a 1D laminar flame code [14] with information about the flame temperature and rate of production of SiO_2 obtained from PREMIX. The flame was burnt at an initial velocity of 144 cm/s at a pressure of 27.5 mbar. The ratio of H_2/O_2 was 1.69 and the ratio of $Ar/(H_2 + O_2)$ was 1.04. A linearly decreasing temperature gradient of -80 K/cm was assumed in accordance with previous simulations [1].

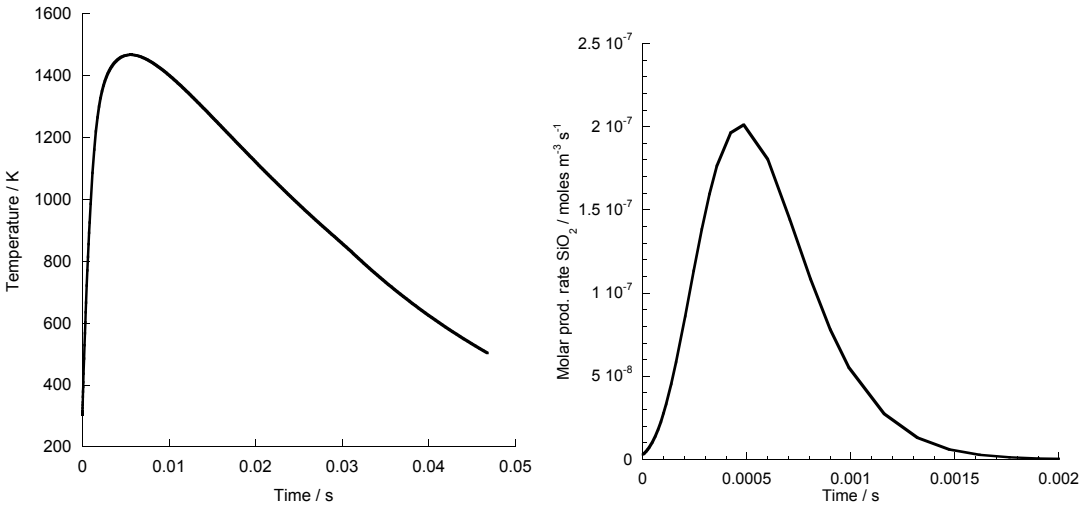

Temperature profile Rate of production profile

Figure 4: Flame parameters calculated by PREMIX.

This data was used as an input for the stochastic simulation. We used 65536 stochastic particles in the simulation and set the initial concentration of particles in the system to zero. The simulation took approximately 10 minutes to complete during which time $\sim 10^8$ jump events were performed.

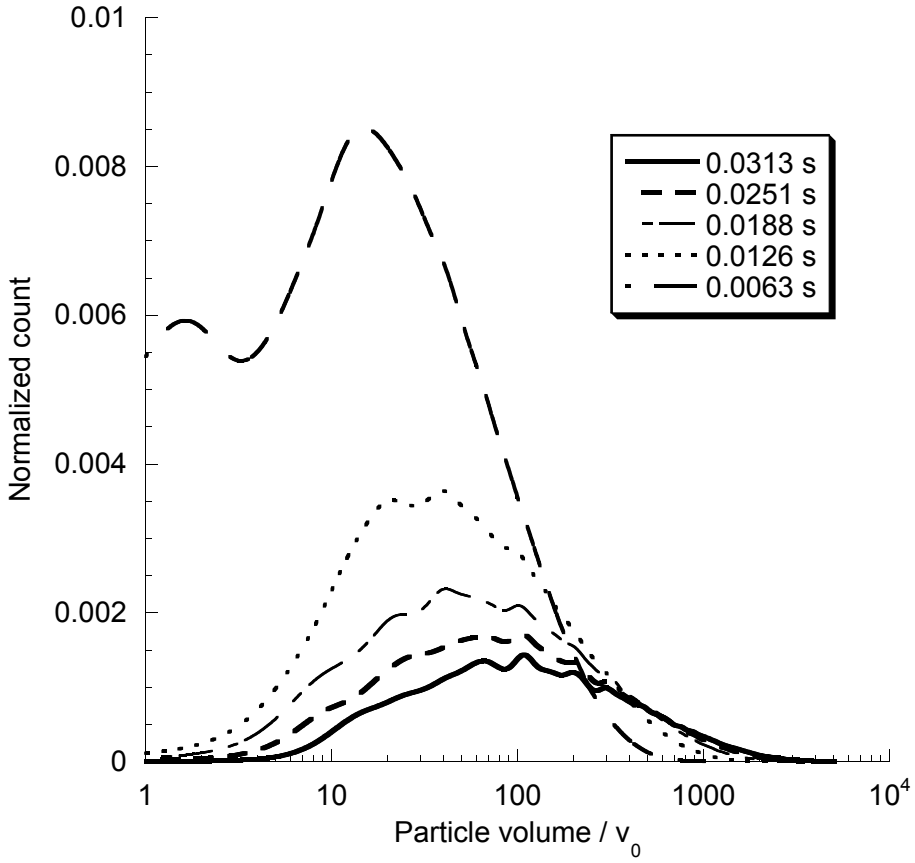

Figure 5: Volume PSD of silica at various times.

Figure 5 shows the evolution of the volume distribution of the silica particles. At early times ($t = 0.0063\,\mathrm{s}$) a bimodal distribution is formed. The first peak is due to small particles from the inception phase still being present in large numbers, whilst the second peak is due to larger coalesced particles. Advancing forward through time, the distribution broadens and becomes unimodal as the smaller particles coagulate with the larger ones.

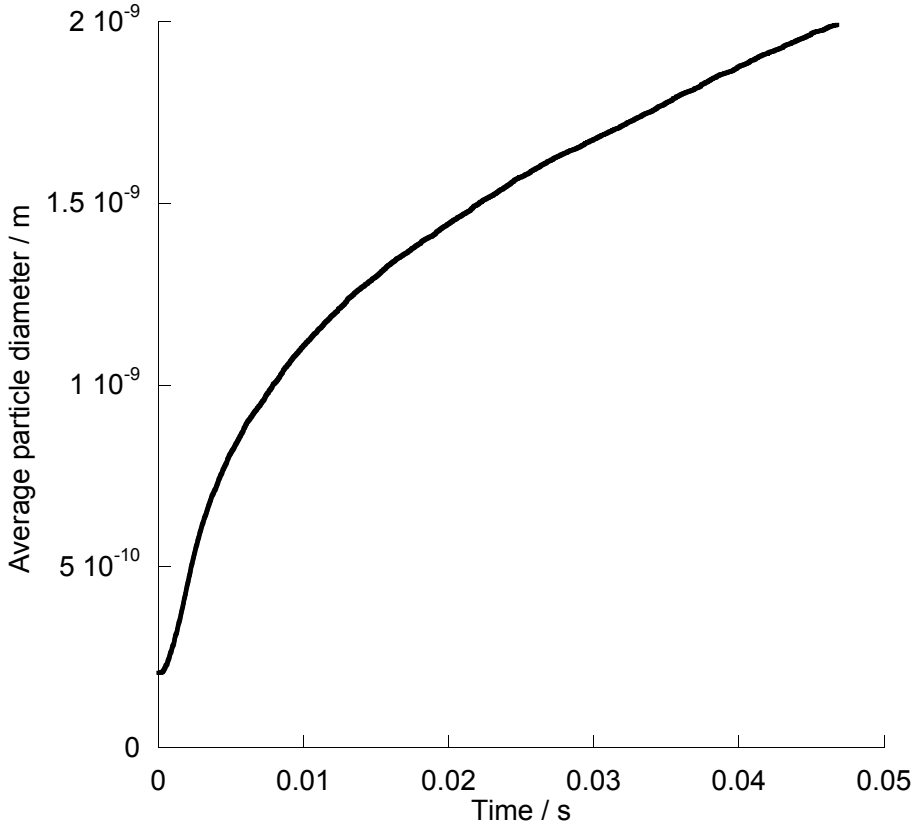

Figure 6: Time evolution of average particle diameter.

Figure 6 shows that the average particle diameter, as calculated using the method described in section 2, rapidly increases at the start of the flame and slows towards the end as the temperature decreases. Finally, Fig. 7 shows to what extent the particles have sintered within the flame. At very early times (Fig. 7(a)) Nearly all the particles lie on the line of complete sintering where $a \propto v^{2/3}$. As the particles progress further through the flame where the temperature drops, the larger particles start to move from the line of complete coalescence (Figs 7(b) and 7(c)). This behaviour is explained by the form of the characteristic sintering time, which increases with particle diameter to the fourth power and is proportional to temperature. At the end of the flame where the temperature has fallen to 503 K we see that the

particles lie mainly off the line of complete coalescence. If we put a line of best fit through the data at 503 K we obtain an average value for the fractal dimension of the particles as calculated from

$$D_f = \frac{2\log(v/v_0)}{\log(a/a_0)}, \tag{16}$$

of $D_f = 2.57$ which is consistent with experimental observations [1].

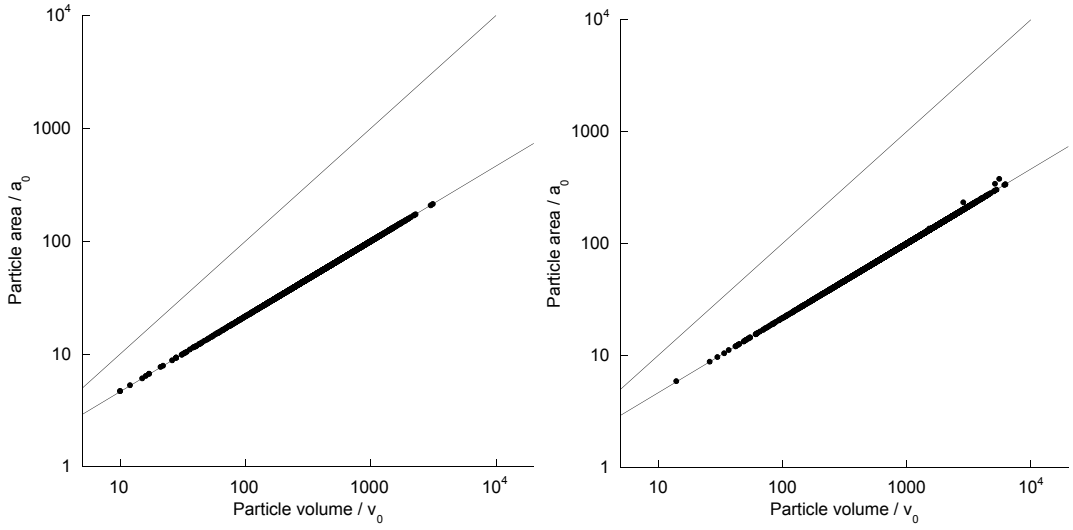

(a) $t = 0.0117\,\mathrm{s}$, $T = 1358\,\mathrm{K}$

(b) $t = 0.0264\,\mathrm{s}$, $T = 1026\,\mathrm{K}$

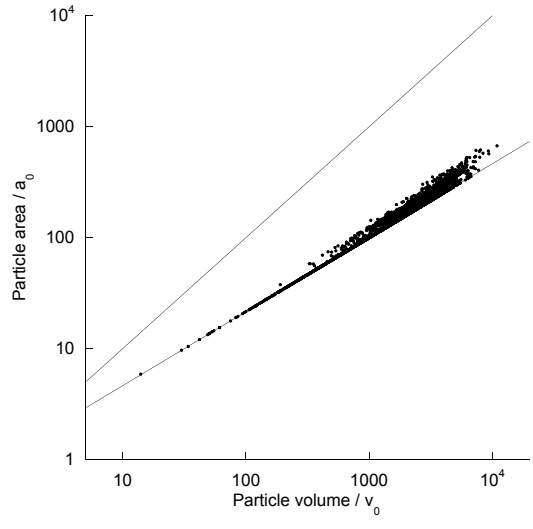

(c) $t = 0.0351\,\mathrm{s}$, $T = 730\,\mathrm{K}$

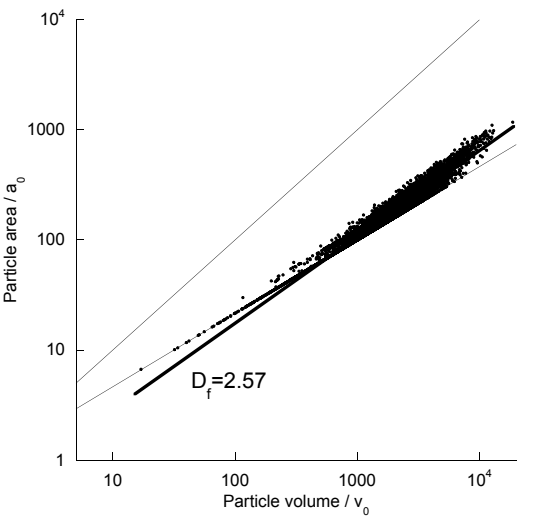

(d) $t = 0.0468\,\mathrm{s}$, $T = 503\,\mathrm{K}$

Figure 7: Surface area vs volume at various temperatures within the flame.

5 Conclusions

A generalization of Smoluchowski's coagulation equation was applied to the growth of nanoparticles in premixed laminar flames. A stochastic mass-flow algorithm was used to compute numerical solutions to this model. The algorithm was then used to simulate a premixed $H_2/O_2/Ar$ flame doped with SiH_4 to produce silica. The PSD of the particles shows a bimodal distribution at early times that changes into a unimodal distribution at later times. The rate of sintering was such that nearly all particles were fully sintered in the flame. In addition to this a value for the fractal dimension, D_f, of the particles was calculated to be 2.57 which is consistent with experimental data.

6 Acknowledgements

The authors would like to thank the the Oppenheimer Fund for the support of Clive Wells and the EPSRC (grant number GR/R85662/01) for the financial support of Neal Morgan under the title 'Mathematical and Numerical Analysis of Coagulation-Diffusion Processes in Chemical Engineering'.

References

[1] D. Lindackers, M.G.D. Strecker, P. Roth, C. Janzen, and S.E. Pratsinis. Formation and growth of SiO_2 particles in low pressure $H_2/O_2/Ar$ flames doped with SiH_4. *Combustion Science and technology*, 123:287–315, 1997.

[2] P.T. Spicer, O. Chaoul, S. Tsantilis, and S.E. Pratsinis. Titania formation by $TiCl_4$ gas phase oxidation, surface growth and coagulation. *Journal of Aerosol Science*, 33:17–34, 2002.

[3] H. Mühlenweg, A. Gutsch, A. Schild, and S.E. Pratsinis. Process simulation of gas-to-particle-synthesis vis population balances: Investigation of three models. *Chemical Engineering Science*, 57:2305–2322, 2002.

[4] P. Tandon and D.E. Rosner. Monte carlo simulation of particle aggregation and simultaneous restructuring. *Journal of Colloid and Interface Science*, 213:273–286, 1999.

[5] C.G. Wells and M. Kraft. Direct simulation and mass flow stochastic algorithms to solve a sintering-coagulation equation. *Preprint c4e 10, Department of Chemical Engineering, University of Cambridge*, 2002.

[6] N.M. Morgan, C.G. Wells, M. Kraft, and W. Wagner. Modelling nanoparticle dynamics: Coagulation, sintering, particle inception and surface growth. *Preprint c4e 19, Department of Chemical Engineering, University of Cambridge*, 2003.

[7] H. Babovsky. On a monte carlo scheme for smoluchowski's coagulation equation. *Monte Carlo Methods and Applictions*, 5(1):1–18, 1999.

[8] A. Eibeck and W. Wagner. An efficient stochastic algorithm for studying coagulation dynamics and gelation phenomena. *SIAM Journal of Scientific Computing*, 22(3):802–821, 2000.

[9] A. Kolodko and K. Sabelfeld. Stochastic particle methods for smoluchowski coagulation equation: variance reduction and error estimations. *Monte Carlo Methods and Applications*, 9(4):315–339, 2004.

[10] A.H. Marcus. Stochastic coalescence. *Technometrics*, 10:133–148, 1968.

[11] A.A. Lushnikov. Some new aspects of coagulation theory. *Izv. Akad. Nauk SSSR Ser. Fiz. Atmosfer. i Okeana*, 14:738–743, 1978.

[12] Y. Xiong and S.E. Pratsinis. Formation of agglomerate particles by coagulation and sintering - part i. a two-dimensional solution of the population balance equation. *Journal of Aerosol Science*, 24(3):283–300, 1992.

[13] N.M. Morgan, C.G. Wells, M.J. Goodson, M. Kraft, and W. Wagner. A new numerical approach for the simulation of the growth of inorganic nanoparticles. *Preprint c4e 22, Department of Chemical Engineering, University of Cambridge*, 2004.

[14] J. Kee, K. Grcar, M.D. Smooke, and J.A. Miller. Premix: A fortran program for modelling steady laminar one-dimensional premixed flames. *SANDIA National Laboratories*, SAND85-8240, 1985.